赤澤智宏、高坂新一.	末梢神経の再生におけるソニックヘッジホッグの役割	BRAIN and NERVE	59	1341-1346	2007
Setsuie, R., Wang, Y. L., Mochizuki, H., Osaka, H., Hayakawa, H., Ichihara, N., Li, H., Furuta, A., Sano, Y., Sun, Y. J., *et al.*	Dopaminergic neuronal loss in transgenic mice expressing the Parkinson's disease-associated UCH-L1 I93M mutant.	*Neurochem Int.*	50(1)	119-129	2007
Osaka H, Ogiwara I, Mazaki E, Okamura N,Yamashita S, Iai M, et al.	Patients with a sodium channel alpha 1 gene mutation show wide phenotypic variation.	*Epilepsy Res*	75	46-51	2007
Tohyama J, Akasaka N, Osaka H, Maegaki Y, Kato M, Saito N, et al.	Early onset West syndrome with cerebral hypomyelination and reduced cerebral white matter.	*Brain Dev*			*in press*
Hirano R, Interthal H, Huang C, Nakamura T, **Deguchi K**, Choi K, Bhattacharjee MB, Arimura K, Umehara F, Izumo S, Northrop JL, Salih MAM, **Inoue K,** Armstrong DL, Champoux JJ, Takashima H, Boerkoel CF	Spinocerebellar ataxia with axonal neuropathy: consequence of a Tdp1 recessive neomorphic mutation?	*EMBO J*	26	4732-43	2007

Deguchi K, Clewing JM, Elizondo LI, Hirano R, Huang C, Choi K, Sloan EA, Lücke T, Marwedel KM, Powell RD, SantaCruz K, Willaime-Morawek S, **Inoue K**, Lou S, Northrop JL, Kanemura Y, van der Kooy D, Okano H, Armstrong DL, Boerkoel CF.	Neurological phenotype of Schimke immuno-osseous dysplasia and neurodevelopmental expression of SMARCAL1	*J Neuropath Exp Neurol*			in revision
Deguchi K, Takashima S, Armstrong DL, Inoue K.	Brains of extremely premature infants with white matter injury also exhibit altered neural progenitor cells and cortical development.	In preparation			

研究成果の刊行物・別刷（抜粋）

Human Molecular Genetics, 2007, Vol. 16, No. 24 **3037–3046**
doi:10.1093/hmg/ddm262
Advance Access published on September 13, 2007

Translation of *SOX10* 3′ untranslated region causes a complex severe neurocristopathy by generation of a deleterious functional domain

Ken Inoue[1,2,*], Tomoko Ohyama[2], Yosuke Sakuragi[1], Ryoko Yamamoto[1], Naoko A. Inoue[1], Yu Li-Hua[1], Yu-ichi Goto[1], Michael Wegner[3] and James R. Lupski[2,4,5]

[1]Department of Mental Retardation and Birth Defect Research, National Institute of Neuroscience, National Center of Neurology and Psychiatry, Tokyo 187-8502, Japan, [2]Department of Molecular and Human Genetics, [3]Institut für Biochemie, Emil-Fischer-Zentrum, Universität Erlangen, Erlangen D-91054, Germany, [4]Department of Pediatrics, Baylor College of Medicine and [5]Texas Children's Hospital, Houston 77030, TX

Received June 11, 2007; Revised and Accepted September 7, 2007

Peripheral demyelinating neuropathy, central dysmyelinating leukodystrophy, Waardenburg syndrome and Hirschsprung disease (PCWH) is a complex neurocristopathy caused by *SOX10* mutations. Most PCWH-associated *SOX10* mutations result in premature termination codons (PTCs), for which the molecular mechanism has recently been delineated. However, the first mutation reported to cause PCWH was a disruption of the native stop codon that by conceptual translation extends the protein into the 3′ untranslated region (3′-UTR) for an additional 82 residues. In this study, we sought to determine the currently unknown molecular pathology for the SOX10 extension mutation using *in vitro* functional assays. Despite the wild-type SOX10 coding sequence remaining intact, the extension mutation led to severely diminished transcription and DNA-binding activities. Nevertheless, it showed no dominant-negative interference with wild-type SOX10 *in vitro*. Within the 82-amino acid tail, an 11-amino acid region (termed the WR domain) was responsible primarily for the deleterious properties of the extension. The WR domain, presumably forming an α-helix structure, inhibited SOX10 transcription activities if inserted in the carboxyl-terminal half of the protein. The WR domain can also affect other transcription factors with a graded effect when fused to the carboxyl termini, suggesting that it probably elicits a toxic functional activity. Together, molecular pathology for the *SOX10* extension mutation is distinct from that of more common PTC mutations. Failure to properly terminate *SOX10* translation causes the generation of a deleterious functional domain that occurs because of translation of the normal 3′-UTR; the mutant fusion protein causes a severe neurological disease.

INTRODUCTION

Mutations in the *SOX10* gene, encoding a transcription factor, that is essential for neural crest development and myelin formation both in the central and peripheral nervous systems (CNS and PNS) (1), are associated with two distinct 'neurocristopathies'. A milder more restricted spectrum trait, Waardenburg–Hirschsprung disease (WS4, OMIM: 277580) combines Waardenburg syndrome and Hirschsprung disease (2), whereas a more severe and complex neurological trait, peripheral demyelinating neuropathy, central dysmyelinating leukodystrophy, Waardenburg syndrome and Hirschsprung disease (PCWH, OMIM: 609136) reveals additional de-/dysmyelinating phenotypes in the PNS and CNS (3–7). The vast majority of disease-associated *SOX10* mutations result in premature termination codons (PTCs), causing either WS4 or PCWH depending on the position of the mutations. The exon position of the PTC is directly associated with a sensitivity or resistance to mRNA degradation by nonsense-mediated mRNA decay (NMD) (3). Functional analyses

*To whom correspondence should be addressed at: Department of Mental Retardation and Birth Defect Research, National Institute of Neuroscience, National Center of Neurology and Psychiatry, 4-1-1 Ogawahigashi-cho, Kodaira, Tokyo 187-8502, Japan. Tel: +81-42-346-1713; Fax: +81- 42-346-1743; Email: kinoue@ncnp.go.jp

indicated that WS4 resulted from *SOX10* haploinsufficiency because the WS4-associated mutant *SOX10* mRNAs contain PTCs in the upstream exons that are subject to rapid degradation by activating the NMD surveillance pathway. In contrast, PCWH is caused by dominant-negative *SOX10* alleles because NMD is unable to detect PCWH-associated mutant mRNAs typically carrying PTCs in the last exon, thereby allowing stable translation of truncated proteins that can interfere with the wild-type SOX10 protein.

However, the first *SOX10* mutation found in a PCWH patient did not result in a PTC. It was a 12 bp deletion (designated as 1400del12) that only disrupted the normal stop codon, presumably leading to an extended in-frame translation into the 3′ untranslated region (3′-UTR) (5). As a result, an additional 82 amino acids are attached to the carboxyl terminus of the normal SOX10 protein creating a mutant fusion protein. Because of the severe neurological phenotype (i.e. PCWH) associated with this extension mutation, it is unlikely that the extension simply causes a loss-of-function allele. However, the exact molecular pathoetiology for this extension mutation remains unknown. Here, we examined the functional properties of the 1400del12 extension mutant by *in vitro* functional assays. Within this extension tail, we identified an 11 amino acid region, that is responsible for the pathologic properties of the mutant protein; i.e. dramatically diminished SOX10 DNA-binding and transcription activities. Furthermore, this domain probably forms an α-helical functional unit and also diminishes transcription activity of SOX9 and SOX11 with a graded effect. In summary, our findings suggest that the extension mutation conveys the severe neurological phenotype by a pathologic function, that is, distinct from PTC mutations, possibly mediated by a gain-of-function effect.

RESULTS

The extension mutant affects SOX10 transcription activities

We previously hypothesized that the proline-rich region within the 82-amino acid extension tail may confer an additional function to the adjacent transactivation domain (5). We surmised that proline may change the native protein structural conformation and the proline-rich region of the SOX10 extension has a moderate homology to one of the proline-rich domains of Wilms tumor 1 transcription factor, a potent transcriptional repression domain (5). We thus tested this hypothesis using *SOX10* expression plasmids carrying the 82-amino acids extension (S mutant, pCMV.SOX10.S) and an extension lacking 19 residues of proline-rich region (D mutant, pCMV.SOX10.D) (Figures 1B and 6).

First, we determined the subcellular localization of these extension mutant proteins by immunocytochemistry using Cos7 cells transiently transfected with *SOX10* expression plasmids (Fig. 1A). Similar to the wild-type and truncated Q250X SOX10 proteins, both of which predominantly localized to the nucleus, SOX10 protein with either the S or D extension is present in the nucleus. In the SOX10 protein, two nuclear localization signals (NLSs) are present flanking the high mobility group (HMG) domain (8). SOX10 also contains one nuclear export signal (NES) within the HMG domain (8). Although SOX10 normally shuttles between the nucleus and the cytoplasm, it is predominantly observed in the nucleus, because the rate of import probably exceeds the rate of export (8). In agreement with the fact that the NLS and NES are maintained in all mutants examined in this study, the extension mutants localized to the nucleus, suggesting that the extensions did not affect the subcellular localization.

Next, we determined whether the extension tail can affect the SOX10 transcription activity by luciferase reporter assays. Wild-type and mutant *SOX10* expression plasmids were transiently transfected into U138 human glioblastoma cells with a luciferase reporter plasmid containing either a synthetic SOX-responsive minimal promoter (3xSXluc) (9) or the human *GJB1* promoter (pGL3-GJB1) (10), that is, directly regulated by *SOX10*. In comparison to the wild type, transcriptional activity of the S extension mutant was dramatically diminished regardless of the promoter utilized to drive expression of the reporter (Fig. 1C showing results for *GJB1* promoter; Data for minimal promoter were not shown), suggesting that the extension completely inactivated the SOX10 transcriptional activity. Interestingly, removal of the proline-rich region from the extension tail did not restore the transcriptional activity, indicating that, contrary to our initial prediction, this proline chain is dispensable for the pathological nature of the extension.

We then examined whether the extension affects the DNA-binding capability of SOX10 protein by electrophoretic mobility shift assay (EMSA). Surprisingly, both S and D extension clones dramatically diminished the DNA-binding ability, despite the fact that the DNA-binding domain is located physically far from the extension in the primary sequence (Fig. 1D). These findings suggest that the extension may involve complex pathologic mechanisms including a major change in structural conformation.

SOX10 harbors a transactivation domain at the carboxyl terminus, that is essential for its transcriptional activity (11). Because the extension tail is located adjacent to the transactivation domain, we examined if the extension can affect the transactivation capability directly and independently. We isolated the carboxyl-terminal region of *SOX10* with extension from the HMG DNA-binding domain and amino-terminal side of the SOX10 protein, and fused it to a POU DNA-binding motif of mouse POU3F1, that is essential for DNA binding and nuclear localization, but not for transcriptional activation (12). In contrast to the prominent activation of over 15-fold by the wild-type SOX10/POU chimera (POU.C354), no activation was observed for fusion constructs with the extension tail (POU.S and POU.D), regardless of the presence or absence of the proline-rich chain (Fig. 1E). These findings suggest that the extension tail also diminishes the transactivation ability of SOX10. These results reveal that the extension mutant dramatically affects SOX10 transcriptional activity, DNA-binding ability and transactivation activity.

Identification of the critical region for the toxicity of the extension

We sought to determine if the pathogenic function of the extension mutant is conveyed by a specific protein sequence motif with functional properties, or is non-specifically determined

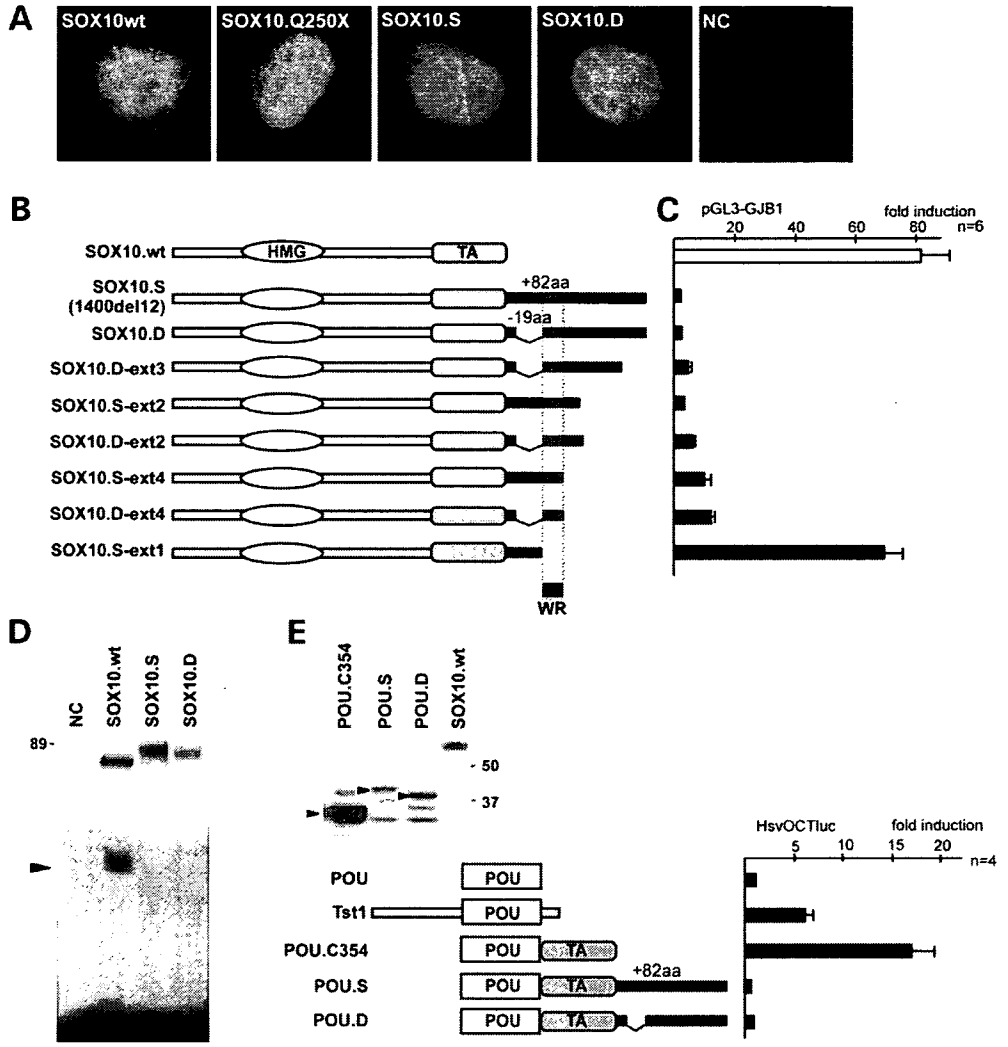

Figure 1. Subcellular localization (**A**) and *in vitro* functional assays (**B**–**E**) of SOX10 extension mutants. (A) Immunocytochemistry using SOX10 antibody shows nuclear localization of wild type, truncated mutant (Q250X), and extension mutant (S and D) SOX10 proteins. An empty vector (pCMV5) was used as a negative control (NC). (B) SOX10 extension mutants used in the assays. Filled bars at the C terminus indicate various lengths of extensions. Black rectangle below and light shade over each clone indicate the position of the WR domain. HMG, high mobility group DNA-binding domain; TA, transactivation domain. (C) Transcription activities determined by luciferase reporter assays. The luciferase reporter plasmid pGL3-GJB1 was used. The *y*-axis corresponds to the clones in (B); the *x*-axis shows the luciferase activities as the relative induction above the mean activity from transfections with luciferase reporter and empty expression plasmid, which was arbitrarily set at 1. (D) DNA-binding assay. SOX10 proteins in nuclear extracts from HeLa cells transfected with wild type (wt) or mutant SOX10 expression plasmids, shown in the western blot (top), were utilized for EMSA (bottom). As a negative control (NC), HeLa cells transfected with an empty vector (pCMV5) was used. SOX10 monomer-binding probe from *MPZ* was used. A molecular weight marker 89 kDa is shown on left. An arrowhead indicates specific binding to the target DNA. (E) Transcription activities determined by luciferase reporter assays using POU/SOX10 fusion plasmids, listed on left, and HsvOCTluc reporter plasmid. Expression of each plasmid was confirmed by western blotting using HeLa cell extract and anti-SOX10 antibody, as shown on top (arrowheads indicate specific signals, and size markers for 37 and 50 kDa are shown on right). The *x*-axis shows the luciferase activities as the relative induction above the mean activity from transfections with luciferase reporter and empty expression plasmid, which was set at 1. In (C) and (E), bars indicate mean ± s.d.

by the physical length of extension and not dependant on particular protein sequences. We generated a series of carboxyl-terminal deletions based on S and D clones, as shown in Fig. 1B, and examined their transcriptional activities by luciferase reporter assays. Among these six deletion clones, only S-ext1, which carries a 23 amino acid extension including the proline-rich region, revealed full transcriptional activity, again showing that the proline-rich region is not responsible for pathogenicity (Fig. 1C). Meanwhile, the other five clones similarly resulted in a large reduction of activity. Although there was a slight tendency for transcriptional activities to inversely increase with a decrease in length of the extension from S to D-ext4 clones, the major change in the activity (>6-fold) from D-ext4 (15 amino acid extension) to S-ext1 (23 amino acid extension) was not likely associated with the difference in the length of the extension.

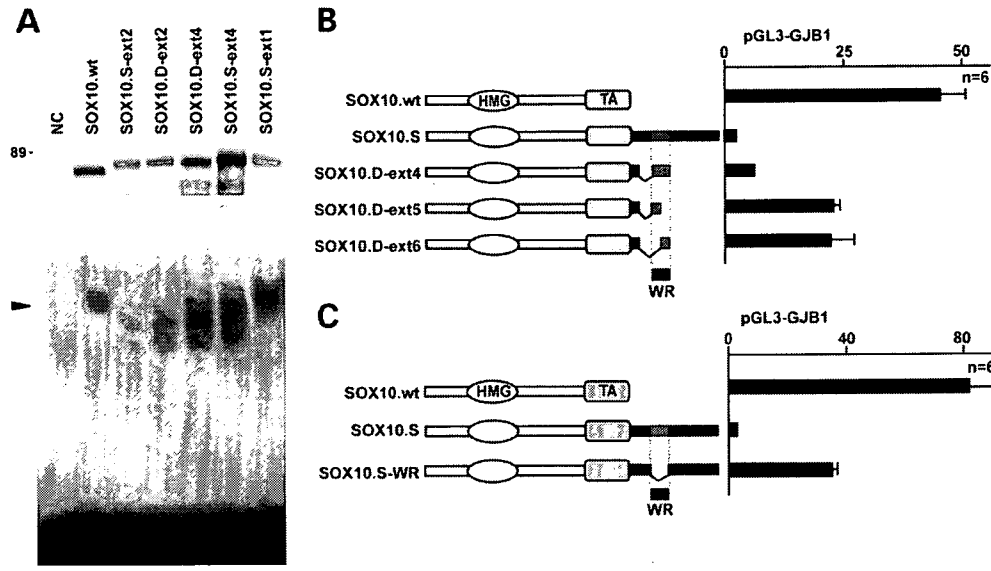

Figure 2. Functional determination of the WR domain. (**A**) DNA-binding assay using SOX10 proteins with different length of extension. SOX10 proteins in nuclear extracts from HeLa cells transfected with wild type (wt) or mutant SOX10 expression plasmids (listed in Fig 1B), shown in the western blot (top), were utilized for EMSA (bottom). As a negative control (NC), HeLa cells transfected with an empty vector (pCMV5) was used. High-affinity SOX10 monomer-binding probe from *MPZ* was used. A molecular weight marker 89 kDa is shown on left. An arrowhead indicates specific binding to the target DNA. (**B** and **C**) Transcription activities determined by luciferase reporter assays using SOX10 extension plasmids, listed on left, and pGL3-GJB1 reporter plasmid. Filled bars at the C terminus indicate various lengths of extensions. Black rectangle below and light shade over each clone indicate the position of the WR domain. HMG, high mobility group DNA-binding domain; TA, transactivation domain. The *x*-axis shows the luciferase activities as the relative induction above the mean activity from transfections with luciferase reporter and empty expression plasmid, which was arbitrarily set as 1. In (B) and (C), bars indicate mean ± s.d.

Comparison of the contents of each clone revealed that the presence of an 11 amino acid region is likely sufficient to diminish the transcriptional activity. The 11 amino acid region consists of WWWQWRRLRRL, enriched by tryptophan in the first half and by arginine in the latter half, thus we designated it as a 'WR domain' (Fig. 1B). EMSA using five of these clones showed that extension mutants with diminished transcriptional activity had defective DNA-binding ability, whereas the S-ext1 clone retained adequate DNA-binding affinity (Fig. 2A), suggesting that the WR domain is sufficient to diminish the DNA binding of the extension mutants.

To further characterize the WR domain, we determined if this 11 amino acid domain can be minimized to a smaller functional unit and yet retain pathogenicity. We removed each half of this domain from the D-ext1 clone, resulting in D-ext5 (carrying WWWQW) and D-ext6 (carrying RRLRRL), respectively (Fig. 2B). Both constructs resulted in a transcriptional up-regulation of 3-fold compared with D-ext4, leading to a restoration of transcriptional activity to half the wild type. These findings suggested that the 11 amino acids probably forms a minimal functional unit to effectively elicit the transcriptional toxicity. Furthermore, elimination of the WR domain from the S extension (designated as S-WR, Fig. 2C) up-regulated the activity by 10-fold, effectively restoring the transcriptional activity to half the wild type. These findings indicated that the WR domain is critical to the toxic function of the extension mutant, although the rest of the extension excluding the WR domain can also suppress the SOX10 activity to some extent.

Inhibitory effect of the inserted WR domain within the SOX10 protein

To determine if the toxicity of the WR domain is position-specific, we inserted this WR domain into various positions of the SOX10 protein (Fig. 3A). These positions were selected so as not to disrupt either the HMG or transactivation domains of SOX10. As controls, we inserted a 10 amino acid myc tag (EQKLISEEDL) at the same positions. Luciferase reporter assays using the *GJB1* reporter revealed that the WR domain, but not the myc tag, diminished the SOX10 transcriptional activity when it was placed downstream of the HMG domain (Fig. 3B). Data obtained using the minimal promoter (3xSXluc) conveyed similar results (data not shown). The inhibitory effect was strong at the *Nae*I and *Dra*III sites and modest at the *Pst*I site. Because, insertion of the myc tag at the same positions did not reduce the transcriptional activity, the inhibitory effect of the WR domain insertion is likely specific to its sequence content. In contrast, both the WR and myc insertions at the *Nar*I site upstream of the HMG domain conveyed an inhibitory effect, wherein the WR insertion showed a milder inhibition. This inhibition by myc insertion at the *Nar*I site was not observed when the minimal promoter was used (data not shown), suggesting that the effect of the insertions at this position may be different among different promoters.

Accordingly, EMSA showed that the WR domain insertions, but not the myc insertions, in the carboxyl-terminal half of the protein resulted in a diminished DNA-binding ability (Fig. 3C), suggesting that the WR domain specifically

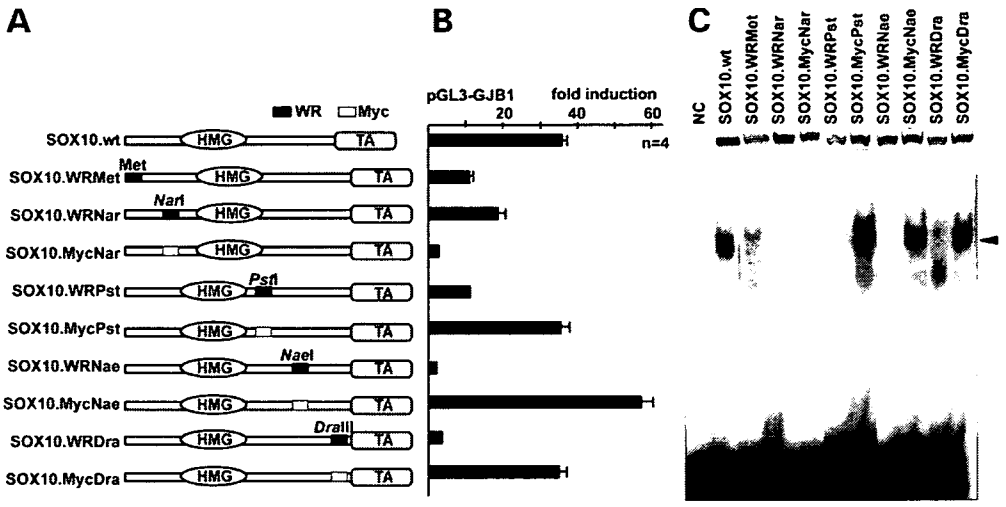

Figure 3. Functional analyses of WR domain insertions. (**A**) SOX10 mutants used in the assays. Black rectangles indicate the WR domain insertions whereas grey rectangles indicate the myc tag insertions. Positions of insertion are shown as initial methionine (Met) and restriction enzyme recognition sites (*NarI*, *PstI*, *NaeI* and *Dra*III). HMG, high mobility group DNA-binding domain; TA, transactivation domain. (**B**) Transcription activities determined by luciferase reporter assays using SOX10 plasmids, listed in (A), and pGL3-GJB1 reporter plasmid. The *x*-axis shows the luciferase activities as the relative induction above the mean activity from transfections with luciferase reporter and empty expression plasmid, which was arbitrarily set as 1. Bars indicate mean ± s.d. (**C**) DNA-binding assay using SOX10 proteins listed in (A). SOX10 proteins in nuclear extracts from HeLa cells transfected with wild type (wt) or mutant *SOX10* expression plasmids with either WR domain or myc insertion, shown in the western blot (top), were utilized for EMSA (bottom). As a negative control (NC), HeLa cells transfected with an empty vector (pCMV5) was used. SOX10 monomer-binding probe from *MPZ* was used. An arrowhead indicates specific binding to the target DNA.

affected the binding to the target. Insertions upstream of the HMG domain also resulted in reduced DNA-binding affinity, however, these may not be sequence specific. Because the *Nar*I insertion is located within the amino acid 61–100 region that immediately precedes the HMG domain and modulates DNA binding of SOX10 in a site-specific manner (13), the insertion may have changed the affinity to the SOX10-binding sequences present in the different probe and promoters used in the EMSA and reporter assays. Nevertheless, these findings demonstrated that the WR domain can also affect the SOX10-binding and transcriptional activities from different positions within the protein.

No dominant-negative interference with the wild-type SOX10 protein

To examine whether the SOX10 mutant proteins with extension can possibly interfere with the wild-type SOX10 protein, we performed competition assays. None of the extension mutants that harbor diminished transcription activity by itself inhibited the activity of the co-present wild-type SOX10, an observation in sharp contrast to the Q250X truncated SOX10 that elicited dominant-negative interference (Fig. 4). As predicted, S-ext1 showed an additive effect, because it retains transcription activity similar to the wild-type SOX10. These findings suggest that, at least in this experimental setting *in vitro*, extension mutants do not function as dominant-negative alleles by competing with the wild-type SOX10.

WR polypeptide inhibited SOX11, SOX9 and POU3F1 transcription activities with a graded effect

If the WR domain has a specific toxic property, it may also be able to affect other transcription factors. We thus examined the effects of the WR domain when fused to two other SOX family member proteins, SOX9 and SOX11, and to a POU domain transcription factor, POU3F1. Again, the myc tag was used as a control. Addition of the WR domain in SOX9, that belongs to the same group as SOX10 (group E), resulted in a ~70% reduction of activity on the SOX-responsive minimal reporter 3xSXluc, but only 30% reduction on the *GJB1* native promoter pGL3-GJB1 (Fig. 5A). Meanwhile, the WR domain dramatically affected SOX11, which belongs to a different subclass (group C) (1), on both minimal and *GJB1* reporters (Fig. 5B). In contrast, both myc and WR domain diminished the POU3F1 activity to one-third, thus the WR domain did not confer specific effects on POU3F1 in comparison with the addition of the myc tag (Fig. 5C). EMSA showed that, unlike SOX10, the WR domain did not confer major changes in the DNA-binding ability of SOX9, SOX11 or POU3F1. Together, the WR domain can also affect transcription factors other than SOX10 with a graded effect, being strong for SOX10 and SOX11, intermediate for SOX9 and similar to the myc tag for POU3F1. These effects may be conveyed by a toxic function of the WR domain. One should note that these findings are not readily applicable to the disease-causing mutations in *SOX9*, *SOX11* or *POU3F1*, because no naturally occurring mutations in theses genes may result in the WR domain due to the sequence divergence in their 3′-UTRs.

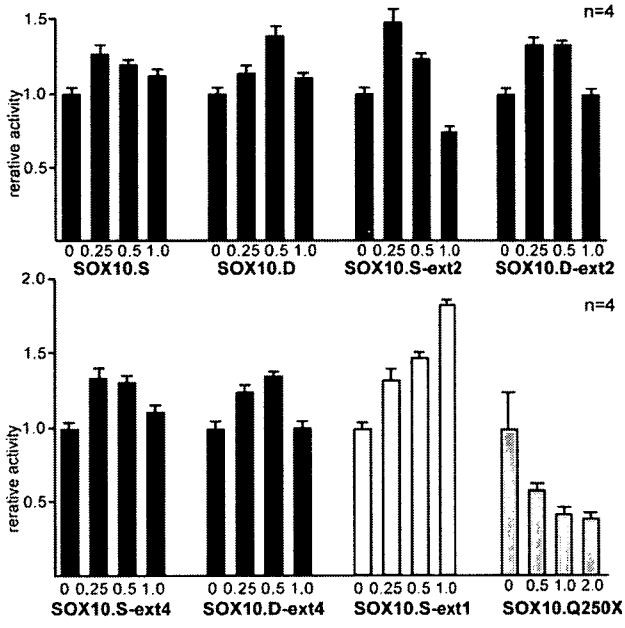

Figure 4. Competition assays. Increasing amounts of mutant *SOX10* expression plasmid were mixed with a fixed amount of wild-type *SOX10* expression plasmid and co-transfected with the luciferase reporter plasmid 3xSXluc. The *x*-axis shows the relative amount of mutant *SOX10* plasmid to the fixed wild-type *SOX10* plasmid. The total amount of DNA per well was kept constant by adding empty expression plasmid. The mean activity from transfections with the luciferase reporter and wild-type *SOX10* plasmid was set as 1, and other data are shown relative to this activity. SOX10.S-ext1 (empty bars) retains transcription activity alone, whereas six SOX10 mutants with filled bars show diminished transcription activity, as shown in Fig 1B. Nevertheless, none of the extension mutants showed dominant-negative interference as demonstrated in SOX10.Q250X truncated mutant (shaded bars). Bars indicate mean ± s.d.

Computational analyses suggest that the WR domain may form an α helix

Our findings strongly suggest that the WR domain may have functional properties that are essential for the pathologic mechanism of the extension mutant. To further delineate such properties and potentially relate them to structural features, we performed computational predictions for the extension region using various protein prediction programs, including SAM-T02 (14), through the ExPASy proteomics server (http://www.expasy.org/) (15).

Multiple secondary structural prediction analyses indicated that the WR domain may form a strong α helix structure (Fig. 6). No other region in the extension tail is predicted to form an apparent secondary structure. Examination and computational analyses of the entire extension showed two other findings: a moderate similarity to type II small proline-rich proteins identified by BLASTP and potential phosphorylation sites predicted by NetPhos (data not shown). However, the WR domain was not directly involved in these features.

DISCUSSION

In this study, we delineated the molecular pathology of a unique *SOX10* extension mutation that was found in the first PCWH patient (5) by *in vitro* functional analyses. The mutation, a 12 bp deletion starting from the second nucleotide of the native stop codon, presumably leads to a failure to properly terminate translation. As a result, by conceptual translation a putative 82-amino acid tail translated from the 3′-UTR was attached to the native carboxyl terminus of intact SOX10 protein sequence creating a mutant fusion protein (5). There is one other *SOX10* mutation with a similar extension with 86 amino acids resulting from substitution of the stop codon to lysine (X467K) (16). Although little information about the neurological examination was available for this case, the baby with this mutation showed mental and global developmental delay in addition to Waardenburg syndrome and Hirschsprung disease, suggesting that the patient probably had PCWH rather than WS4. Thus, the in-frame *SOX10* extensions are likely associated with PCWH.

Our luciferase reporter assays and EMSA demonstrated that, despite the wild-type SOX10 protein sequence remaining intact, the additive extension completely diminished the transcriptional activity both on the minimal and *GJB1* promoters, suggesting that extension may elicit deleterious effects. Because loss-of-function of one allele, or haploinsufficiency, of *SOX10* is associated with a WS4 phenotype, whereas the extension mutations cause more severe PCWH phenotype, it is unlikely that the extension mutant simply acts as a loss-of-function allele. Our competition assays demonstrated that the extension mutants do not interfere with co-present wild-type SOX10 activity, indicating that dominant-negative action is less likely, at least in our *in vitro* experimental setting. Nevertheless, these findings are not readily applicable *in vivo* without further experimental validation. Interestingly, one study reported an enhanced transcription activity of the extension mutant (1400del12) (17). We were unable to clarify the reason for this discrepancy. This study also reported reduced transcription activity for the PCWH-causing X467K mutant with an in-frame 86 amino acid extension. This latter finding is rather consistent with our results.

We found that the deleterious effect of the extension is primarily associated with a specific functional domain that plays a critical role. Within the 82-amino acid extension tail our studies using a series of deletion constructs identified an 11 amino acid region, that we termed the WR domain, to be responsible for the deleterious function. Although the WR domain polypeptide sequence does not have homology to any known proteins or functional motifs, it consists of α-helix secondary structure with high probability, which may structurally form a functional unit. Indeed, our experimental findings suggest structural effects of the WR domain. First, insertions of the WR domain at different positions specifically disrupted the DNA-binding and transcription activities only when it was placed downstream of the HMG domain. Second, WR domain attachment also affected SOX9 and SOX11 with a graded effect, but only conferred non-specific inhibition on POU3F1. Because secondary and tertiary structural predictions of the SOX10 protein revealed that the HMG DNA-binding domain is comprised of three α-helix units, while other regions appear to form no major secondary structure, we hypothesize that the α-helix WR domain may interfere with the HMG domain in a structurally specific manner. Further investigation of this currently unknown mol-

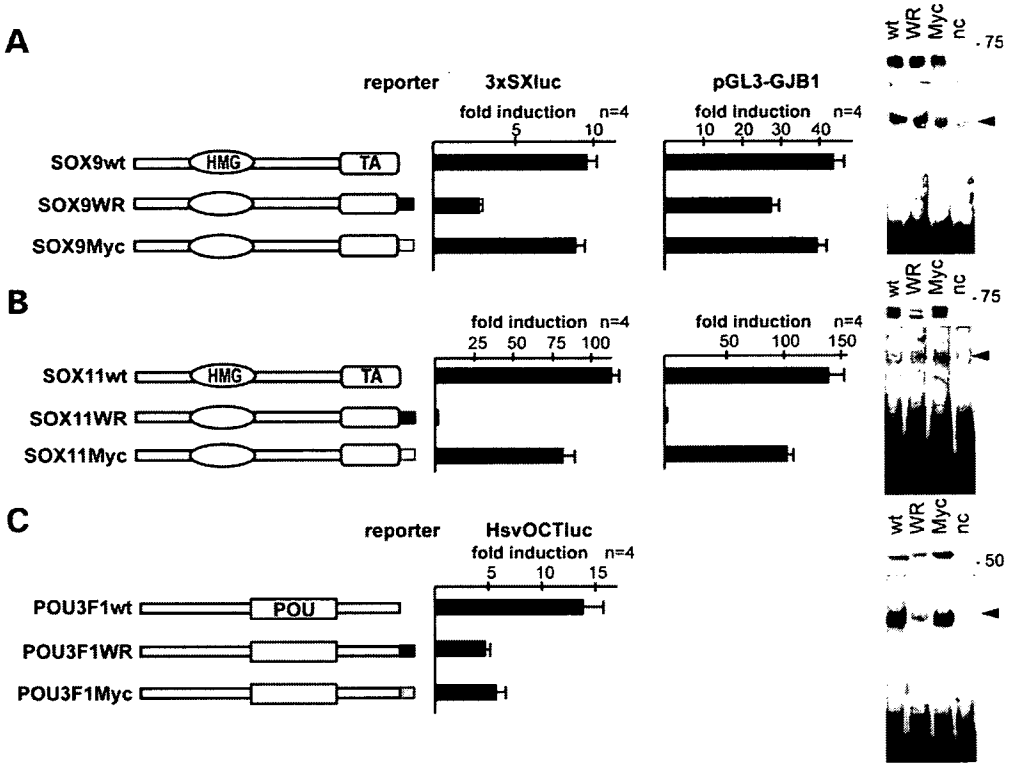

Figure 5. Inhibitory effects of the WR domain on other transcription factors. Transcription activities were determined by luciferase reporter assays using *SOX9* (**A**), *SOX11* (**B**) and *POU3F1* (**C**) plasmids, as listed on left. Black rectangles indicate the WR domain insertions whereas grey rectangles indicate the myc tag insertions. Each expression plasmid was co-transfected with either 3xSxluc (middle) or pGL3-GJB1 (right) reporter plasmid for SOX protein and HsvOCT reporter plasmid for POU3F1 protein. The *x*-axis shows the luciferase activities as the relative induction above the mean activity from transfections with luciferase reporter and empty expression plasmid, which was arbitrarily set as 1. Bars indicate mean ± s.d. DNA- binding assays and western blottings using each protein listed on left were shown on right. Protein extracts from Cos7 cells transfected with wild type (wt), WR, Myc or empty vector (negative control, nc) plasmid, shown in the western blot (top), were utilized for EMSA (bottom). SOX-binding probe was used for SOX9 and SOX11, whereas POU-binding probe was utilized for POU3F1. Molecular weight markers 75 or 50 kDa are shown on right. Arrowheads indicate specific binding to the target DNA.

ecular mechanism for the potential interaction between the WR domain and HMG domain will help clarify the pathologic basis for the toxic effect of the WR domain.

Disruption of the native stop codon without changing wild-type protein coding sequence is an uncommon cause for human genetic diseases. More frequent frame-shift mutations in the coding sequences can give rise to similar 'out-of-frame' translations, but the impact of such 'out-of-frame' tails in the disease pathoetiology probably differs case by case, depending on location of the frame-shift alteration, reading frame (i.e. one base plus or two bases plus), or actual DNA sequences comprising the coding and non-coding region of a gene, as we previously demonstrated in the myelin protein zero; *MPZ*, gene (18). In fact, at least four disease-causing frame-shift mutations have been reported in *SOX10*, namely 778delG, 795delG, 847insT and 1076delGA, resulting in 25, 19, 10 and 41 amino acid extension tails, respectively (2,3,6,19,20). Clinical severity conveyed by these mutations appears to be associated with the location of PTCs (i.e. the more proximal the truncation is located, the more severe the phenotype), but not with the length, position or protein sequence of the 'out-of-frame' tails. Of note, 1076delGA mutation, which produces the longest tail, was associated with WS4 in a family; no PCWH-associated neurological symptoms were apparent and consequently no dominant-negative interference was observed by functional assays (3). Theses findings further support the unique toxic property of the WR domain that is only conveyed by in-frame translation of the SOX10 3′-UTR.

Collectively, our *in vitro* functional analyses showed that molecular pathogenesis for PCWH caused by extension mutations is distinct from that caused by PTC mutations. We determined that the WR domain within the extension probably elicited a functional property that is responsible for the toxicity of the extension, thus causing the PCWH phenotype. Although the exact nature of this toxicity is not fully delineated yet, it probably acts through a gain-of-function mechanism.

With these findings, now the genotype–phenotype correlation of *SOX10* mutations has been consolidated. Loss-of-function alleles are associated with a milder and more restricted spectrum trait, WS4, in which no de-/dysmyelinating phenotypes in the PNS and CNS are involved. In contrast, dominant-negative alleles, mainly resulting from common

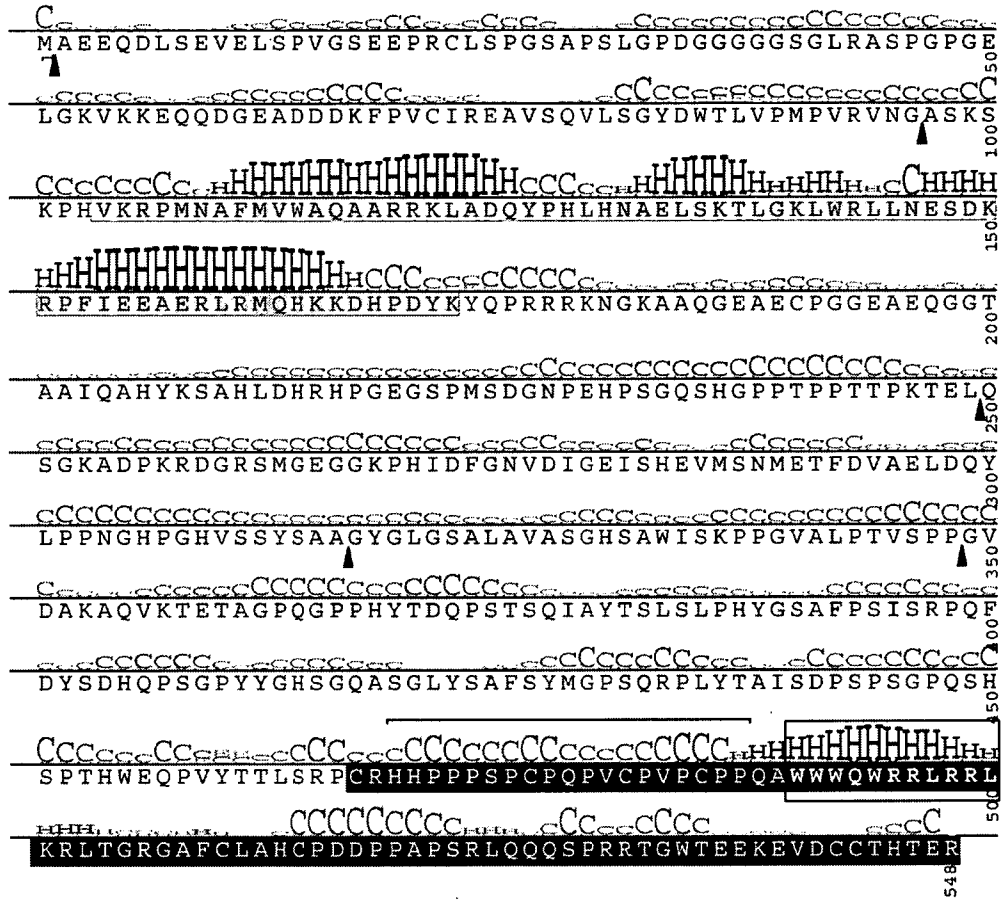

Figure 6. Predicted secondary structure of SOX10 protein with the 82-amino acid extension. Data obtained by SAM-T02 protein structure prediction program (14) are summarized. Predicted secondary structure is shown above the protein sequence for the SOX10 extension mutant. H, α helix; E, β bridges and strands; C, others including coils. The height of the letter represents the likelihood of the prediction. Shaded sequences indicate HMG domain that consists of three blocks of α helix, and the sequences written in white show the 82-amino acids extension. A rectangle indicates the WR domain, showing an α helix structure. A horizontal line indicates the proline-rich 19-amino acids region deleted in SOX10.D extension mutant. Arrowheads show the position of either WR domain or myc tag insertion indicated in Fig 3A.

PTC mutations, and gain-of-function alleles, conveyed by rare extension mutations as demonstrated in this study, give rise to more severe and complex trait, PCWH.

MATERIALS AND METHODS

Construction of expression plasmids

Human *SOX10* cDNA was inserted into a mammalian expression plasmid pCMV5 under the control of a cytomegalovirus promoter, as described (3,9). Various mutations were incorporated by PCR or PCR-based site-directed mutagenesis. Resultant mutants were: pCMV.SOX10.S that carries the 1400del12 mutation, pCMV.SOX10.D that lacks the proline-rich 19 amino acid region (HHPPPSPCPQPVCPVPCPP; see Fig. 6 for the actual location), and a 3′ end deletion series as shown in Figures 1B and 2B, designated as pCMV.SOX10.S-ext1 to pCMV.SOX10.D-ext6. The carboxyl-terminal half of *SOX10* that contains the transactivation domain was fused to a POU cassette of rat POU3F1, that contains a DNA-binding domain and nuclear localization signal, to generate pCMV.POU.C354(11), pCMV.POU.S and pCMV.POU.D (Fig. 1E). An 11 amino acid sequence (WWWQWRRLRRL; designated as the WR domain) or a myc tag (EQKLISEEDL) was inserted at various positions within the SOX10 protein (Figures 3A and 6). The WR domain was removed from pCMV.SOX10.S to generate pCMV.SOX10.S-WR (Fig. 2C). The WR domain or myc tag was inserted in frame before the stop codon of rat *SOX11*, mouse *SOX9* and mouse *POU3F1* cDNA in the pCMV5 expression plasmid to generate WR or myc fusion constructs (Fig. 5).

Immunocytochemistry

Cos7 cells were grown on chamber slides in DMEM medium supplemented with 10% fetal bovine serum (FBS) and transiently transfected with *SOX10* expression plasmids using Poly-Fect transfection reagent (Qiagen, Germany). Cells were fixed

in 4% paraformaldehyde in PBS for 5 min, then washed and permeabilized with 0.1% Tween 20 in PBS for 5 min. After twice rinsing with PBS, cells were blocked with 5% normal goat serum at room temperature for 1 h and incubated with rabbit anit-SOX10 antibody (1:500 dilution; Chemicon, CA, USA) at 4°C overnight, followed by two washes with PBS and incubation with AlexaFluor488 goat anti-rabbit antibody (1:5000: Invitrogen, CA, USA) for 1 h at room temperature before visualization by standard fluorescent microscopy. For nuclei staining, an AntiFade Kit with 4′,6′-diamidino-2-phenylindole (Invitrogen) was used.

Transfection assays using luciferase reporter system

Two SOX10-responsive luciferase reporter plasmids, 3xSXluc and pGL3-GJB1 [termed pGL3-Cx32 in our previous study (3)], and one POU-responsive reporter plasmid, HsvOCTluc, were prepared as described previously (3,9,10). U138 human glioblastoma cells were grown in DMEM medium supplemented with 10% FBS and were transiently transfected using PolyFect or Lipofectamine2000 (Invitrogen) transfection reagents. We selected U138 for these studies specifically because it does not express endogenous SOX10 protein that might interfere with transfection assays (9). A total of 0.5–0.8 μg of plasmid DNA per well was used. Typically, we used 0.2 μg reporter plasmid, 0.2 μg test plasmid and 0.1 μg inner control plasmid per well. We collected cells from 24-well trays after 48 h of transfection and assayed luciferase activity using a monolight luminometer (Pharmingen, CA, USA) or TD-20/20 luminometer (Promega, WI, USA). A β-galactosidase expression plasmid, pCMVβ (Clontech, CA, USA), or *Renilla* luciferase expression plasmid, pRT-TK (Promega), were used as a reference for transfection. Each experiment was repeated at least three times with at least four independent samples per experiment. Representative results from one experiment were shown in figures.

Western blotting and EMSA

HeLa cells were grown in DMEM medium supplemented with 10% FBS. Nuclear extract was obtained from HeLa cells after 48 h of transfection (21), which was used for western blotting and EMSA. Rabbit antibody to SOX10 (1:3000 dilution) was used for western blots. Other antibodies utilized were: goat anti-SOX9 antibody (Santa Cruz P-20, 1:500 dilution), guinea pig anti-SOX11 antibody (1:3000 dilution) (22) and goat anti-POU3F1 antibody (Santa Cruz H-13, 1:500 dilution). A 15 bp probe containing the high-affinity monomer *SOX10*-binding site found in *MPZ* gene promoter (site B) (23) or 29 bp probe containing POU-binding site (HsvOCT) (9) was used for EMSA, as described previously (3). We selected this *MPZ SOX10* monomer-binding probe, rather than *GJB1* dimer-binding site, due to its simplicity, its well-characterized property and its strong binding affinity (13,23). EMSA was performed using either ^{32}P-labeled or biotin-labeled probes.

Computational analyses

We determined structural and functional characteristics of the SOX10 mutant proteins by a series of web-based prediction programs, primarily available through the ExPASy proteomics web server (http://www.expasy.org/).

ACKNOWLEDGEMENTS

We thank Dr Chihiro Akazawa for his helpful discussions and Dr Kimiko Deguchi for her suggestions and support. This study was supported in part by following grants from the Japanese Ministry of Health, Labor, and Welfare, research grant for Nervous and Mental Disorders (19A-5), and Health and Labor Science Research Grant, Japan (H18-Kokoro-Ippan-015, KI); from the Japanese Ministry of Education, Culture, Sports, Science and Technology Grant-in-Aid for Scientific Research (17390102 to K.I.); from U.S. National Institute for Neurological Disorders and Strokes, U.S. National Institute of Health grant (RO1 NS27042 to J.R.L.).

Conflict of Interest statement. None declared.

REFERENCES

1. Wegner, M. and Stolt, C.C. (2005) From stem cells to neurons and glia: a Soxist's view of neural development. *Trends Neurosci.*, **28**, 583–588.
2. Pingault, V., Bondurand, N., Kuhlbrodt, K., Goerich, D.E., Préhu, M.O., Puliti, A., Herbarth, B., Hermans-Borgmeyer, I., Legius, E., Matthijs, G. *et al.* (1998) *SOX10* mutations in patients with Waardenburg-Hirschsprung disease. *Nat. Genet.*, **18**, 171–173.
3. Inoue, K., Khajavi, M., Ohyama, T., Hirabayashi, S., Wilson, J., Reggin, J.D., Mancias, P., Butler, I.J., Wilkinson, M.F., Wegner, M. *et al.* (2004) Molecular mechanism for distinct neurological phenotypes conveyed by allelic truncating mutations. *Nat. Genet.*, **36**, 361–369.
4. Inoue, K., Shilo, K., Boerkoel, C.F., Crowe, C., Sawady, J., Lupski, J.R. and Agamanolis, D.P. (2002) Congenital hypomyelinating neuropathy, central dysmyelination, and Waardenburg-Hirschsprung disease: phenotypes linked by *SOX10* mutation. *Ann. Neurol.*, **52**, 836–842.
5. Inoue, K., Tanabe, Y. and Lupski, J.R. (1999) Myelin deficiencies in both the central and the peripheral nervous systems associated with a *SOX10* mutation. *Ann. Neurol.*, **46**, 313–318.
6. Pingault, V., Guiochon-Mantel, A., Bondurand, N., Faure, C., Lacroix, C., Lyonnet, S., Goossens, M. and Landrieu, P. (2000) Peripheral neuropathy with hypomyelination, chronic intestinal pseudo-obstruction and deafness: a developmental 'neural crest syndrome' related to a SOX10 mutation. *Ann. Neurol.*, **48**, 671–676.
7. Touraine, R.L., Attié-Bitach, T., Manceau, E., Korsch, E., Sarda, P., Pingault, V., Encha-Razavi, F., Pelet, A., Augé, J., Nivelon-Chevallier, A. *et al.* (2000) Neurological phenotype in Waardenburg syndrome type 4 correlates with novel *SOX10* truncating mutations and expression in developing brain. *Am. J. Hum. Genet.*, **66**, 1496–1503.
8. Rehberg, S., Lischka, P., Glaser, G., Stamminger, T., Wegner, M. and Rosorius, O. (2002) Sox10 is an active nucleocytoplasmic shuttle protein, and shuttling is crucial for Sox10-mediated transactivation. *Mol. Cell. Biol.*, **22**, 5826–5834.
9. Kuhlbrodt, K., Herbarth, B., Sock, E., Hermans-Borgmeyer, I. and Wegner, M. (1998) Sox10, a novel transcriptional modulator in glial cells. *J. Neurosci.*, **18**, 237–250.
10. Bondurand, N., Girard, M., Pingault, V., Lemort, N., Dubourg, O. and Goossens, M. (2001) Human Connexin 32, a gap junction protein altered in the X-linked form of Charcot-Marie-Tooth disease, is directly regulated by the transcription factor SOX10. *Hum. Mol. Genet.*, **10**, 2783–2795.
11. Kuhlbrodt, K., Schmidt, C., Sock, E., Pingault, V., Bondurand, N., Goossens, M. and Wegner, M. (1998) Functional analysis of Sox10 mutations found in human Waardenburg-Hirschsprung patients. *J. Biol. Chem.*, **273**, 23033–23038.
12. Sock, E., Enderich, J., Rosenfeld, M.G. and Wegner, M. (1996) Identification of the nuclear localization signal of the POU domain protein Tst-1/Oct6. *J. Biol. Chem.*, **271**, 17512–17518.

13. Peirano, R.I. and Wegner, M. (2000) The glial transcription factor Sox10 binds to DNA both as monomer and dimer with different functional consequences. *Nucleic Acids Res.*, **28**, 3047–3055.
14. Karchin, R., Cline, M., Mandel-Gutfreund, Y. and Karplus, K. (2003) Hidden Markov models that use predicted local structure for fold recognition: alphabets of backbone geometry. *Proteins*, **51**, 504–514.
15. Gasteiger, E., Gattiker, A., Hoogland, C., Ivanyi, I., Appel, R.D. and Bairoch, A. (2003) ExPASy: the proteomics server for in-depth protein knowledge and analysis. *Nucleic Acids Res.*, **31**, 3784–3788.
16. Sham, M.H., Lui, V.C.L., Chen, B.L.S., Fu, M. and Tam, P.K.H. (2001) Novel mutations of *SOX10* suggest a dominant negative role in Waardenburg-Shah syndrome. *J. Med. Genet.*, **38**, E30.
17. Chan, K.K., Wong, C.K., Lui, V.C., Tam, P.K. and Sham, M.H. (2003) Analysis of *SOX10* mutations identified in Waardenburg-Hirschsprung patients: differential effects on target gene regulation. *J. Cell. Biochem.*, **90**, 573–585.
18. Khajavi, M., Inoue, K., Wiszniewski, W., Ohyama, T., Snipes, G.J. and Lupski, J.R. (2005) Curcumin treatment abrogates endoplasmic reticulum retention and aggregation-induced apoptosis associated with neuropathy-causing myelin protein zero-truncating mutants. *Am. J. Hum. Genet.*, **77**, 841–850.
19. Pingault, V., Girard, M., Bondurand, N., Dorkins, H., Van Maldergem, L., Mowat, D., Shimotake, T., Verma, I., Baumann, C. and Goossens, M. (2002) *SOX10* mutations in chronic intestinal pseudo-obstruction suggest a complex physiopathological mechanism. *Hum. Genet.*, **111**, 198–206.
20. Shimotake, T., Tanaka, S., Fukui, R., Makino, S. and Maruyama, R. (2007) Neuroglial disorders of central and peripheral nervous systems in a patient with Hirschsprung's disease carrying allelic SOX10 truncating mutation. *J. Pediatr. Surg.*, **42**, 725–731.
21. Andrews, N.C. and Faller, D.V. (1991) A rapid micropreparation technique for extraction of DNA-binding proteins from limiting numbers of mammalian cells. *Nucleic Acids Res.*, **19**, 2499.
22. Potzner, M.R., Griffel, C., Lütjen-Drecoll, E., Bösl, M.R., Wegner, M. and Sock, E. (2007) Prolonged Sox4 expression in oligodendrocytes interferes with normal myelination in the central nervous system. *Mol. Cell. Biol.*, **27**, 5316–5326.
23. Peirano, R.I., Goerich, D.E., Riethmacher, D. and Wegner, M. (2000) Protein zero gene expression is regulated by the glial transcription factor Sox10. *Mol. Cell. Biol.*, **20**, 3198–3209.

ARTICLE IN PRESS

Available online at www.sciencedirect.com

ScienceDirect

ELSEVIER

Biochemical and Biophysical Research Communications xxx (2007) xxx–xxx

BBRC

www.elsevier.com/locate/ybbrc

Endosomal trafficking of EGFR regulated by hVps18 via interaction of MVB sorting machinery

Bong Yoon Kim [a], Chihiro Akazawa [b,*]

[a] *Protein Chemistry Laboratory, School of Biological Sciences, Seoul National University, Seoul 151-742, Republic of Korea*
[b] *Department of Biophysics and Biochemistry, Graduate School of Health Sciences, Tokyo Medical and Dental University, Yushima 1-5-45, Bunkyo-Ku, Tokyo 113-8519, Japan*

Received 2 August 2007

Abstract

Although recent studies have provided important insights into the molecular events underlying endosomal sorting of cargo into multivesicular bodies (MVBs), the precise mechanisms that are responsible for fusion of MVBs with lysosomes remain poorly understood. Here we report the interaction of hVps18, a component of the mammalian Class C Vps/HOPS complex, with TSG101 and Hrs, two key components of the MVB sorting machinery. Specifically, we found that hVps18 interacts with TSG101 and Hrs via the NH_2-terminal coiled-coil domain containing regions and is recruited to endosomes following TSG101 and Hrs expression. In addition, we found that overexpression of hVps18 inhibits the degradation of EGFR, resulting in prolonged activation of downstream signaling cascade pathways. These results suggest that hVps18 play a role not only in fusion and clustering of late endosomes and lysosomes, but also in the regulation of MVB sorting machinery.

Keywords: Class C Vps/HOPS complex; ESCRT; TSG101; Hrs; MVB

Regulated degradation of cell surface receptors is critical for the many biological functions, including cell proliferation, survival, migration, and differentiation [1]. After agonist stimulation, internalized receptor cargo can be delivered either to recycling vesicles for transport back to the cell surface or to lysosomes for degradation. The receptors destined for degradation are sorted within the endosomal system and transferred to the internal vesicles of late endosomes or multivesicular bodies (MVBs), which eventually fuse with lysosomes. These intraluminal vesicles are then degraded by lipases and the associated proteins are degraded by lysosomal proteases [2,3]. Recent studies have shown that monoubiquitination of receptor cargo proteins serves as a sorting signal for targeting to MVB vesicles [4–6]. The molecular mechanism by which ubiquitinated cell surface receptors are selected and targeted for degradation is highly conserved throughout evolution, and occurs from yeast to mammals. The ubiquitinated cargo proteins are recognized by endosomal ubiquitin-binding protein Vps27 in yeast and its homolog hepatocyte growth factor regulated tyrosine kinase substrate (Hrs) in mammals. Vps27/Hrs then binds Vps23, or the mammalian Vps23 homolog tumor susceptibility gene 101 (TSG101), a key component of the endosomal sorting complex required for transport-I (ESCRT-I) complex. The association of Vps27/Hrs and Vps23/TSG101 leads to the recruitment of ESCRT-I and two other downstream ESCRT complexes, ESCRT-II and ESCRT-III, and thus facilitates cargo transport into MVB [4,7,8].

The Class C Vps complex is composed of four proteins, Vps11, Vps16, Vps18, and Vps33. This complex is not only involved in SNARE-mediated membrane fusion at the lysosome-like yeast vacuole, but also plays a role in tethering and docking processes at earlier stages of the vesicle transport pathway, both from the Golgi to endosomes and endosomes to the vacuole [9–13]. They also are components of a large detergent-insoluble homotypic fusion and

* Corresponding author. Fax: +81 42 567 0518.
E-mail address: c.akazawa.bb@tmd.ac.jp (C. Akazawa).

0006-291X/$ - see front matter © 2007 Elsevier Inc. All rights reserved.
doi:10.1016/j.bbrc.2007.08.046

Please cite this article in press as: B.Y. Kim, C. Akazawa, Endosomal trafficking of EGFR regulated by hVps18 via ..., Biochem. Biophys. Res. Commun. (2007), doi:10.1016/j.bbrc.2007.08.046

vacuole protein sorting (HOPS) complex that contains two additional proteins, Vam6 (Vps39) and Vps41 (Vam2) [9,10]. Recently, it has been found that the Class C Vps complex also contributes to a novel new tethering complex involving Vps8 and Vps3, called the Class C core vacoule/endosome tethering (CORVET) complex, which is important in endo-lysosomal biogenesis. The HOPS complex contains Vam6 (Vps39) and Vps41 (Vam2), whereas the CORVET complex contains the Vam6 homolog Vps3 and Vps41 homolog Vps8 [14]. These complexes are structurally and functionally conserved from yeast to mammals. In mammals, the six Class C Vps/HOPS components comprise a large hetero-oligomeric complex that localizes to the endosomal compartment and interacts with multiple SNARE proteins involved in endocytic pathways [15–18]. Previous studies involving RNA interference (RNAi)-mediated depletion of Vps18 or overexpression of mammalian Class C Vps proteins have shown that the mammalian Class C Vps complex regulates endosome/lysosome fusion, clustering, and synaptic transmission in neurons [16–19].

In the course of investigating the functional relationship between mammalian ESCRTs and Class C Vps/HOPS complexes in the late endocytic degradation pathways, we find that hVps18, a component of Class C Vps/HOPS complex, directly interacts with TSG101 and Hrs, two key components of ESCRT complexes in MVB pathway. Moreover, we show that overexpression of hVps18 inhibits endosome to lysosome trafficking of EGFR, resulting in retained activation of a downstream signaling cascade.

Results

hVps18 interacts with TSG101 and Hrs, two components of the multivesicular sorting machinery

As a first step to test the hypothesis that mammalian the Class C Vps/HOPS complex is involved in the regulation of cell surface receptor trafficking for lysosomal degradation and interacts with MVB sorting machinery, we performed yeast two-hybrid interaction assays to assess the ability of Class C Vps/HOPS complex components to bind TSG101 and Hrs, As shown in Fig. 1A, we found that only hVps18, but not hVps11, hVps16, or hVps33a, specifically interacts with TSG101 and Hrs. Two other Class C Vps/HOPS complex components, hVps39 and hVps41, also did not interact with TSG101 and Hrs (data not shown). To confirm these interactions *in vivo*, COS-7 cells were cotransfected with Myc-tagged full-length hVps18 or hVps16 and GFP-tagged full-length TSG101 or Hrs. After transfection, cells were lysed and subjected to immunoprecipitation analysis using anti-GFP antibodies. As shown in Fig. 1B, GFP-tagged full-length TSG101 and Hrs efficiently coimmunoprecipitated Myc-tagged full-length hVps18 (lane 2 and 4), but not Myc-tagged full-length hVps16 (lane 1 and 3).

Taken together, these results indicate that hVps18 specifically interacts with TSG101 and Hrs, two key components of the MVB sorting machinery.

hVps18 colocalizes with TSG101 and Hrs on endosomes

Since hVps18 specifically associated with TSG101 and Hrs (Fig. 1A and B), we performed double immunofluorescence confocal microscopy to examine whether hVps18 colocalizes with TSG101 and Hrs. Consistent with previous reports [20–22], we found that overexpression of GFP-TSG101 or GFP-Hrs induced aberrant, large vesicular structures in the cytoplasm of cells. In contrast, overexpressed Myc-hVps18 or hVps16 were distributed broadly throughout the cytoplasm (data not shown). As shown in Fig. 1C, when HeLa cells were cotransfected with Myc-tagged full-length hVps18 or hVps16 and GFP-tagged TSG101 or Hrs, we observed an altered hVps18 localization found that displayed substantial overlap with GFP-tagged TSG101 and Hrs (Fig. 1C and f, arrows). In contrast, Myc-tagged hVps16 was unaffected by overexpression of GFP-tagged TSG101 or Hrs, and retained a diffuse distribution that did not overlap with either GFP-tagged TSG101 or Hrs (see Supplemental Fig. 1). On the basis of these observations, we conclude that the interactions between hVps18 and Hrs or TSG101 observed by yeast two-hybrid and immunoprecipitation experiments occur in mammalian cells and may be involved in the recruitment of hVps18 to endocytic compartments.

Structural requirements of hVps18 interactions with TSG101 and Hrs

To map the domain(s) involved in the interactions between hVps18 and TSG101 or Hrs, we generated several deletion constructs of TSG101 (Supplemental Fig. 2A), Hrs (Supplemental Fig. 2B), and hVps18 (Fig. 2A). We then analyzed the impact of these deletions on the interaction between hVps18 and TSG101 or Hrs using yeast two-hybrid interaction assays. As shown in Fig. 2A, NH_2-terminal coiled-coil region deleted hVps18 (hVps18Δ1) dramatically decrease the interaction with TSG101ΔN2, while deletions of the COOH-terminal RING-H2/coiled-coil domain and the clathrin heavy chain repeat (CHCR) domain (hVps18 ΔC2–ΔC4) did not affect the interaction with TSG101ΔN3 (Fig. 2A). Conversely, we found that the COOH-terminal region between the coiled-coil and steadiness box (SB) domains of TSG101 (TSG101ΔN2), which comprises residues 311–345, is critical for the interaction with hVps18, while the NH_2-treminal UEV (TSG101ΔC) and COOH-terminal SB domain (TSG101ΔN3) are not required (Supplemental Fig. 2A). Meanwhile, using the same yeast two-hybrid interaction assays, we found that NH_2-terminal end region of hVps18 (hVps18ΔN) is critical for the interaction with the Hrs–UIM containing region (Hrs–UIM) (Fig. 2A). Conversely, the central ubiquitin interacting motif (UIM) containing region (residues 226–416) of Hrs was essential for binding hVps18, while the NH_2-terminal VHS, FYVE domain, and other COOH-terminal portions of Hrs were not required (Supplemental Fig. 2B).

Please cite this article in press as: B.Y. Kim, C. Akazawa, Endosomal trafficking of EGFR regulated by hVps18 via ..., Biochem. Biophys. Res. Commun. (2007), doi:10.1016/j.bbrc.2007.08.046

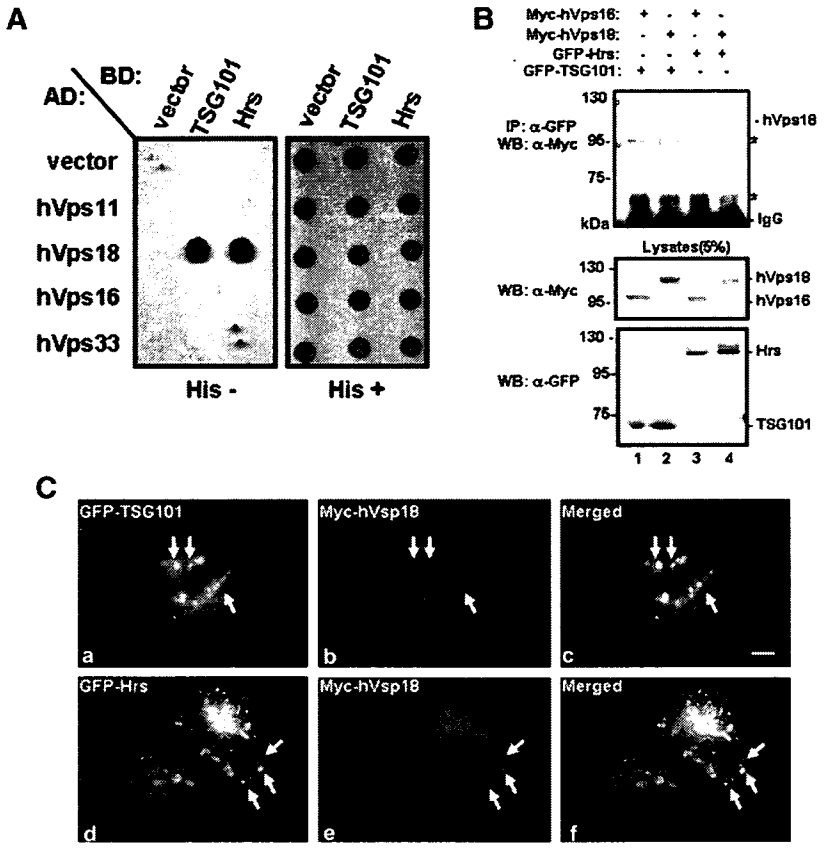

Fig. 1. hVps18 specifically interacts with TSG101 and Hrs. (A) Yeast two-hybrid analyses of the interactions between Class C Vps molecules and TSG101 and/or Hrs. Yeast cells were cotransformed with plasmids encoding the *GAL4* activation domain fused to each full-length Class C Vps molecule and the *GAL4* binding domain fused to TSG101 and Hrs. Cotransformed cells were spotted onto histidine-deficient (His−) or histidine-containing (His+) plates and incubated at 30 °C for 2–3 days. Growth on histidine-deficient (His−) plates is indicative of an interaction between both proteins. (B) Coimmunoprecipitation of Vps18 and TSG101 or Hrs. COS-7 cells were cotransfected Myc-tagged hVps18 and hVps16 with GFP-tagged TSG101 or Hrs as indicated, and subsequently immunoprecipitations were performed using anti-GFP antibodies. Immunoprecipitates were subjected to Western blotting using anti-Myc antibodies. Western blot analysis with anti-GFP and anti-Myc antibodies on the soluble cell lysates prior to immunoprecipitation are also included. (C) Immunofluorescence microscopy analyses of HeLa cells transfected with Myc-Vps18 and GFP-TSG101 (a–c), or GFP-Hrs (d–f). Transfected cells were fixed, permeabilized, and immunostained with a monoclonal antibody to Myc followed by Texas Red-conjugated donkey anti-mouse IgG. GFP-TSG101 and Hrs were directly visualized by GFP fluorescence (green: a,c) and myc-Vps18 (red: b,e). Merged images are represented in the third panel of each row (c,f); the arrows indicate overlapping distributions and colocalization of the proteins. Scale bar represents 10 μm.

To verify these findings biochemically in a mammalian cell system, we performed immunoprecipitation analyses in COS-7 cells transfected with the indicated hVps18 constructs and GFP-tagged TSG101 or Hrs (see Supplemental Fig. 3A and B). Consistent with the results from above yeast two-hybrid analyses, coimmunoprecipitation analyses showed that wild type and Δ2 constructs of hVps18 efficiently coimmunoprecipitated with GFP-tagged TSG101 (Supplemental Fig. 2A, lanes 1 and 2) or Hrs (Supplemental Fig. 3B, lane 1). However, deletion of the hVps18 central coiled-coil domain (hVps18Δ1) and NH_2-terminal end region (hVps18ΔN) completely abolished the interaction with GFP-tagged TSG101 (Supplemental Fig. 3A, lane 3) or Hrs (Supplemental Fig. 3B, lane2).

Taken together, these results show that the central coiled-coil domain and NH_2-terminal end regions of hVps18 are essential for the association with residues 311–345 of TSG101 or the central UIM domain of Hrs, respectively (Fig. 2B).

hVps18 is recruited to TSG101 and Hrs-induced enlarged endosomes via its NH_2-terminal binding region

To confirm these findings more precisely using immunoflourescence microscopy, we performed double immunoflourescence microscopy to examine whether those binding regions of hVps18 are critical for the recruitment of hVps18 to endosomes induced by overexpression of GFP-tagged TSG101 or Hrs. Although the subcellular distribution of the hVps18 deletion mutants is unchanged (data not shown), as we predicted from our yeast two-hybrid and biochemical results (Figs. 1 and 2), in cells coexpressing hVps18Δ1 and GFP-TSG101 or hVps18ΔN and GFP-Hrs that unable to interact with each other, there was no recruitment of Myc-hVps18ΔN and Myc-hVps18ΔC1 to GFP-TSG101 (Fig. 3A, d–f), or GFP-Hrs positive endosomes (Fig. 3B, d–f). In contrast, hVps18Δ2 and GFP-TSG101, or hVps18Δ1 and GFP-Hrs, those com-

Please cite this article in press as: B.Y. Kim, C. Akazawa, Endosomal trafficking of EGFR regulated by hVps18 via ..., Biochem. Biophys. Res. Commun. (2007), doi:10.1016/j.bbrc.2007.08.046

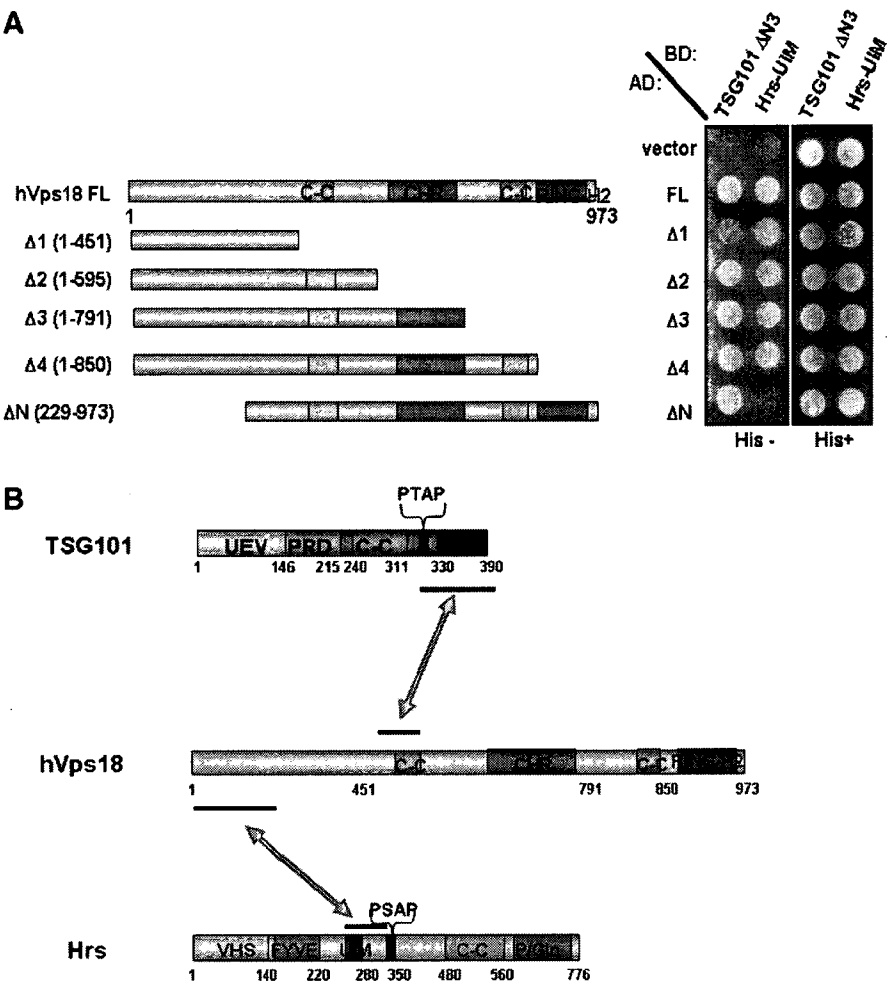

Fig. 2. Identification of hVps18 and TSG101 or Hrs binding sites by deletion analyses. (A) Schematic representation of hVps18 deletion constructs used in this study and yeast two-hybrid analyses of the interaction between hVps18 and TSG101ΔN3, or Hrs–UIM. The following domains of hVps18 are indicated: C-C, coiled-coil; CHCR, clathrin heavy chain repeat; RING-H2, RING-H2 finger. Yeast transformants bearing the combination of constructs indicated were spotted onto media with histidine (His+) or without histidine (His−), respectively. (B) A model illustrating the identified binding sites of hVps18 and TSG101 or Hrs.

binations that are able to interact with each other, display clear recruitment of Myc-hVps18Δ2 to GFP-TSG101-positive endosomes (Fig. 3A, a–c), or Myc-hVps18Δ1 to GFP-Hrs positive endosomes (Fig. 3B, a–c). These results clearly suggest that the recruitment of Myc-tagged full-length hVps18 to endosomes is dependent on its interaction with GFP-Hrs and TSG101 via its NH_2-terminal region.

Overexpression of hVps18 inhibits EGFR degradation

Hrs and TSG101 are critical for epidermal growth factor receptor (EGFR) sorting and trafficking to the lysosome for degradation. Our findings that hVps18 interacts with TSG101 and Hrs prompted us to ask whether hVps18 functions in the sorting and down-regulation of endocytosed EGFR. To address this possibility, we examined whether hVps18 overexpression affects ligand-induced degradation of EGF receptors. COS-7 cells expressing GFP-vector alone or GFP-tagged full-length hVp18 were treated with EGF to induce receptor endocytosis and lysosomal degradation of the receptor. After the indicate time of treatment, cells were lysed, equal amounts of protein separated by SDS–PAGE, and the amount of EGFR quantified by Western blotting with anti-EGFR antibodies. As shown in Fig. 4A and B, EGFR levels significantly decreased in cells transfected with GFP-vector alone after EGF stimulation, consistent with rapid ligand-induced endocytosis, sorting, and lysosomal degradation. In contrast, expression of GFP-tagged hVps18 had strong effect on the steady state levels of EGFR levels and also strongly inhibited EGF-induced EGFR degradation compared with only GFP-vector transfected cells (Fig. 4A and B). Given the critical roles of endosome to lysosome trafficking of EGFR in the attenuation of EGFR signaling [1], we next examined whether the overexpression of hVps18 affects the mitogen-activated kinase-signaling pathway, which is downstream of EGF-

Please cite this article in press as: B.Y. Kim, C. Akazawa, Endosomal trafficking of EGFR regulated by hVps18 via ..., Biochem. Biophys. Res. Commun. (2007), doi:10.1016/j.bbrc.2007.08.046

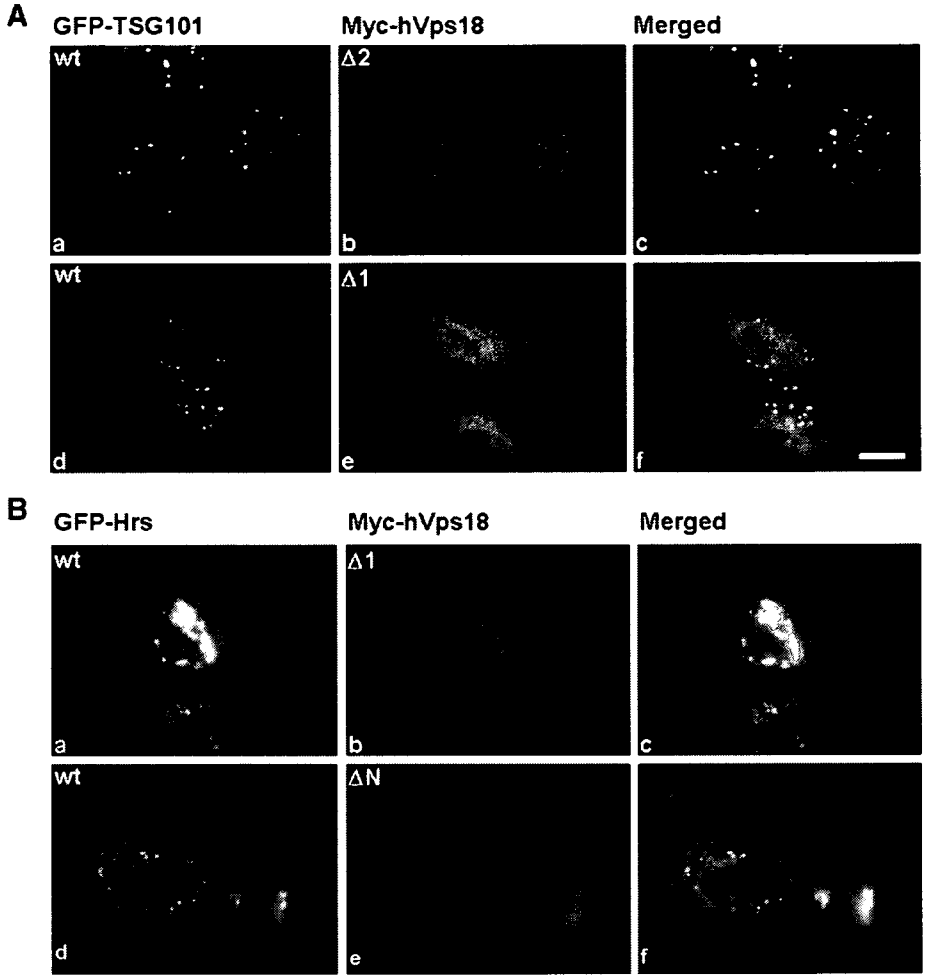

Fig. 3. Recruitment of hVps18 to GFP-TSG101 and Hrs-induced endosomes via NH_2-terminal binding sites. (A) HeLa cells coexpressing GFP-tagged TSG101 and Myc-tagged hVps18Δ1 or hVps18Δ1, were costained with anti-Myc antibodies. (B) HeLa cells coexpressing GFP-tagged Hrs and Myc-tagged hVps18Δ1 or hVps18ΔN were costained with anti-Myc antibodies. GFP-tagged TSG101 and Hrs were directly visualized by GFP-fluorescence. The yellow color indicates colocalization of the proteins. Scale bar represents 10 μm.

activated EGFR. Within 10 min after EGF stimulation, ERK42/44 proteins are strongly phosphorylated in both GFP-vector alone and GFP-hVps18 transfected cells. However, GFP-hVps18 overexpression significantly alters the inactivation phase of ERK42/44 phosphorylation, leading to prolonged activation of the MAP kinase-signaling cascade (Supplemental Fig. 4A and B). These results suggest that hVps18 is required for the degradation of EGFR and the down-regulation of the EGFR-activated MAP kinase-signaling pathway.

Discussion

The lysosome serves as the final destination and degradative compartment for many endocytic, autophagic, and secretory materials targeted for destruction in eukaryotic cells. Therefore, lysosomal degradation is critical to many cellular processes, including the turnover of normal cellular proteins, down-regulation of surface receptors, release of endocytosed nutrients, antigenic processing, etc. [2]. Although many proteins are targeted for lysosomal degradation through the MVB sorting pathway, the molecular mechanisms that regulate the final stages of the fusion events between MVBs and lysosomes remain poorly understood. In this study, our findings demonstrate that hVps18, a component of mammalian Class C Vps/HOPS complex, interacts directly with two components of MVB sorting machinery, TSG101 and Hrs. hVps18 contains highly conserved functional domains, including the CHCR and RING-H2 finger domains, which are both important for recruitment to late endocytic organelles [16]. Interestingly, our yeast two-hybrid analyses show that only the NH_2-terminal regions of hVps18 is necessary for the interaction with TSG101 and Hrs, while the CHCR and COOH-terminal RING-H2 finger motif are not required (Fig. 2 and Supplemental Fig. 3). These results raise the possibility that the association of hVps18 with the Class C Vps/HOPS complex and multivesicular body sorting machinery, such

Please cite this article in press as: B.Y. Kim, C. Akazawa, Endosomal trafficking of EGFR regulated by hVps18 via ..., Biochem. Biophys. Res. Commun. (2007), doi:10.1016/j.bbrc.2007.08.046

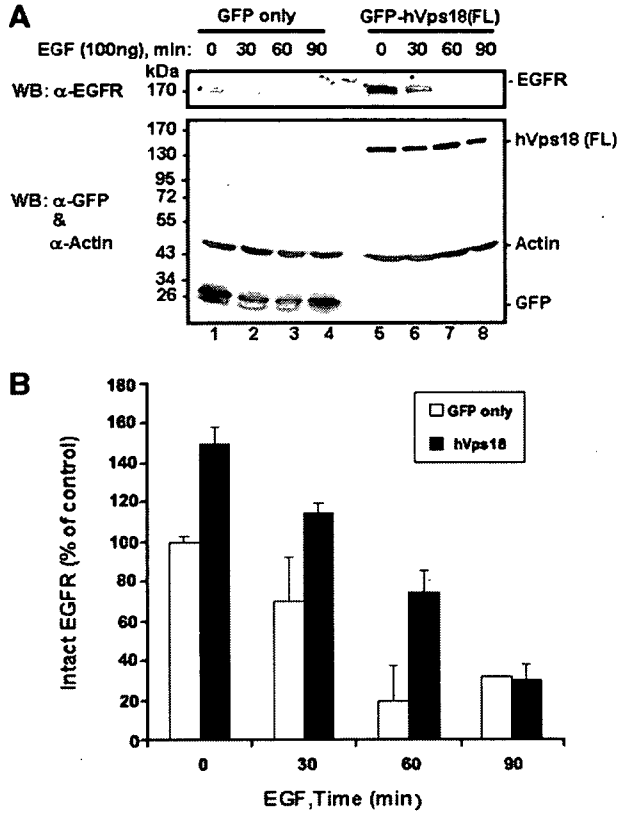

Fig. 4. Overexpression of hVps18 inhibits ligand-induced EGFR degradation and disrupts downstream signaling of EGFR. (A) COS-7 cells transfected with GFP-vector alone or GFP-hVps18 were stimulated with EGF (100 ng/ml) for the indicated times. The cells were lysed and analyzed by Western blotting using antibodies against EGFR and GFP. The same membrane was immunoblotted with anti-actin antibody to verify equal loading. (B) The remaining EGFR level after EGF treatment was quantified and expressed as a percentage of EGFR level in untreated control cells. Data are means + SEM (error bar) of the results from two independents experiments.

as TSG101 and Hrs, is differentially regulated by its domain structures. Moreover, our immunofluorescence microscopic analyses demonstrate that the NH_2-terminal region of hVps18 is critically required for the recruitment of hVps18 to GFP-TSG101 and Hrs-induced enlarged endosomes (Fig. 3A and B). These results strongly support the possibility that described above and suggest a potential role for hVps18 in the MVB sorting pathway. Interestingly, although it has been recently shown that hVps18 has E3 ubiquitin ligase activity and ubiquitinates specific substrates, including Snk and GGA3 [25,26], we did not find any clear ubiquitination of Hrs and TSG101 by hVps18 using an *in vivo* ubiquitination assay (data not shown). Therefore, our data suggest that hVps18 may act as a specific regulator for the MVB sorting machinery at endosomes due to its direct interactions with TSG101 and Hrs, or potentially due to ubiquitination of endocytic substrates after recruitment by TSG101 or Hrs. Consistent with our biochemical and cell biological studies of hVps18 interaction with TSG101 and Hrs, we found that overexpression of hVps18 significantly inhibits EGFR degradation (Fig. 4A and B), resulting in prolonged activation of MAP kinase-signaling cascade (Supplemental Fig. 4A and B). These results are strikingly similar to phenotypes that result from depletion of components of the ESCRT-1, including TSG101 and Vps37A [22–24], suggesting that hVps18 is a regulator of the MVB sorting pathway.

In summary, we report here for the first time the direct interaction of hVps18, a component of mammalian Class C Vps/HOPS complex, with TSG101 and Hrs, two key components of MVB sorting pathway. Although further functional and physiological studies are required to understand the extent of the cellular consequences of these interactions, our findings presented here strongly suggest that hVps18 (or the Class C Vps/HOPS complex) plays a role during the early stages of ubiquitinated cargo sorting through its interactions with TSG101 and Hrs, in addition to roles in membrane fusion and clustering of late endocytic organelles.

Material and methods

Plasmids. The full-length mammalian Class C Vps molecules used in this study have been described previously [15,17]. Human full-length TSG101 and mouse full-length Hrs cDNA were generous gifts from Stanley N. Cohen (Stanford University). For yeast two-hybrid analyses, the full-length mammalian Class C Vps/HOPS molecules were subcloned into pACT2 vector, and Hrs and TSG101 were subcloned into pGBKT7 or pGBT9 vector (Clontech, Palo Alto, CA, USA). The deletion constructs (Fig. 2A–C) for yeast two-hybrid analyses were generated using QuickChange site-directed mutagenesis kits (Stratagene, La Jolla, CA). Full-length and deletion mutants of hVps18, Hrs, or TSG101 cDNAs were subcloned into pCMV-Myc and pEGFP-C2 vector (Clontech, Palo alto, CA, USA) to produce the Myc- and GFP-tagged forms.

Antibodies. Antibodies used in this study include: anti-EGFR, anti-GFP (B-2), anti-actin (I-19), and anti-Myc (9E10) from Santa Cruz Biotechnology; anti-HA (12CA5, Roche Applied Science), anti-ERK42/44, anti-phosphoERK42/44 (Cell Signaling), and secondary antibodies conjugated to horseradish peroxidase (HRP) and Texas Red (TR) (Jackson Immunoresearch Laboratories).

Yeast two-hybrid assays. Transformation of yeast CG1945 cells with the indicated constructs was performed using the lithium acetate method as described previously [22].

Cell transfection and immunoprecipitation. HeLa and COS-7 cells were cultured in Dulbecco's modified Eagles's medium (DMEM) supplemented with 10% (v/v) fetal bovine serum (FBS), 2 mM glutamine, 100 U/ml penicillin, 100 μg/ml streptomycin in 5% CO_2 at 37 °C. Cells were transfected using Metafectamine (Biontex) according to the manufacturer's instructions and immunoprecipitations were carried out with indicated antibodies as described previously [15].

Immunofluorescence microscopy. For the immunofluorescence microscopy, HeLa cells were fixed with 3% paraformaldehyde (PFA) in PBS for 30 min at room temperature and processed for indirect immunofluorescence microscopy as described previously [15]. Cells were mounted using Vectashield (Vector Laboratories, Inc.). Images were acquired using a Zeiss Axioplan II microscope (Applied Precision).

EGFR degradation assays. GFP-vector and GFP-hVps18 transfected COS-7 cells were serum starved for 6 h and then incubated in medium supplemented with or without 100 ng/ml EGF (ProSpec-Tany TechnoGene, Rehovot, Israel) for the indicated times. All procedures were carried out as described previously [22]. The band intensities were quantified using NIH Image (version 1.63).

ERK42/44 phosphorylation assays. GFP-vector and GFP-hVps18 transfected COS-7 cells were starved in serum-free medium for 6 h and

Please cite this article in press as: B.Y. Kim, C. Akazawa, Endosomal trafficking of EGFR regulated by hVps18 via ..., Biochem. Biophys. Res. Commun. (2007), doi:10.1016/j.bbrc.2007.08.046

then treated with 10 ng/ml EGF for 5 min at 37 °C. After washing with acidic solution (150 mM NaCl, 1000 mM glycine, pH 3.0) and then with PBS, cells were chased in serum-free medium for the indicated times at 37 °C. Cell lysates were separated by SDS–PAGE, followed by immunoblotting using anti-ERK42/44 or anti-phospho-ERK42/44 antibodies.

Acknowledgments

We greatly appreciate Dr. James A. Olzmann (Emory University, Atlanta, GA) for critical reading and helpful discussions.

Appendix A. Supplementary data

Supplementary data associated with this article can be found, in the online version, at doi:10.1016/j.bbrc.2007.08.046.

References

[1] H. Waterman, Y. Yarden, Molecular mechanisms underlying endocytosis and sorting of Erb B receptor tyrosine kinases, FEBS Lett. 16 (2001) 142–152.
[2] C. Mullins, J.S. Bonifacino, The molecular machinery for lysosome biogenesis, Bioessays 23 (2001) 333–343.
[3] D.J. Katzmann, G. Odorizzi, S.D. Emr, Receptor down regulation and multivesicular body sorting, Nat. Rev. Mol. Cell Biol. 3 (2002) 893–905.
[4] D.J. Katzmann, M. Babst, S.D. Emr, Ubiquitin-dependent sorting into the multivesicular body pathway requires the functions of a conserved endosomal protein sorting complex, ESCRT-I, Cell 106 (2001) 145–156.
[5] L. Hicke, R. Dunn, Regulation of membrane protein transport by ubiquitin and ubiquitin binding proteins, Ann. Rev. Cell Dev. Biol. 19 (2003) 141–172.
[6] J. Gruenberg, H. Stenmark, The biogenesis of multivesicular endosomes, Nat. Rev. Mol. Cell Biol. 5 (2004) 317–323.
[7] M. Babst, D.J. Katzmann, W.B. Snyder, B. Wendland, S.D. Emr, Endosome-associated complex, ESCRT-II, recruits transport machinery for protein sorting at the multivesicular body, Dev. Cell 3 (2002) 283–289.
[8] M. Babst, D.J. Katzmann, E.J. Estepa-Sabal, T. Meerloo, S.D. Emr, Escrt-III: an endosome associated heterooligomeric protein complex required for MVB sorting, Dev. Cell 3 (2002) 271–282.
[9] A.E. Wumser, T. Sato, S.D. Emr, New component of the vacuolar class C-Vps complex couples nucleotide exchange on the Ypt7 GTPase to SNARE-dependent docking and fusion, J. Cell Biol. 151 (2000) 551–562.
[10] D.F. Seals, G. Eitzen, N. Margolis, W.T. Wickner, A.A. Price, Ypt/Rab effector complex containing the Sec 1 homolog Vps33p is required for homotypic vacuole fusion, Proc. Natl. Acad. Sci. 97 (2000) 9402–9407.
[11] T.K. Sato, P. Rehling, M.R. Peterson, S.D. Emr, Class C Vps protein complex regulates vacuolar SNARE pairing and is required for vesicle docking/fusion, Mol. Cell 6 (2000) 661–671.
[12] A. Srivastava, C.A. Woolford, E.W. Jones, Pep3p/Pep5p complex: a putative docking factor at multiple steps of vesicular transport to the vacuole of *Saccharomyces cerevisiae*, Genetics 156 (2000) 105–122.
[13] M.R. Peterson, S.D. Emr, The class C Vps complex functions at multiple stages of the vacuolar transport pathway, Traffic 2 (2001) 476–486.
[14] K. Peplowska, D.F. Markgraf, C.W. Ostrowicz, G. Bange, C. Ungermann, The CORVET tethering complex interacts with the yeast Rab5 homolog Vps21 and is involved in endo-lysosomal biogenesis, Dev. Cell 12 (2007) 739–750.
[15] B.Y. Kim, H. Kramer, A. Yamamoto, E. Kominami, S. Kohsaka, C. Akazawa, Molecular characterization of mammalian homologues of class C Vps proteins that interact with syntaxin-7, J. Biol. Chem. 276 (2001) 29393–29402.
[16] V. Poupon, A. Stewart, S.R. Gray, R.C. Piper, J.P. Luzio, The role of mVps18p in clustering, fusion, and intracellular localization of late endocytic organelles, Mol. Biol. Cell 14 (2003) 4015–4027.
[17] B.Y. Kim, M. Ueda, E. Kominami, K. Akagawa, S. Kohsaka, C. Akazawa, Identification of mouse Vps16 and biochemical characterization of mammalian class C Vps complex, Biochem. Biophys. Res. Commun. 311 (2003) 577–582.
[18] S.C. Richardson, S.C. Winistorfer, V. Poupon, J.P. Luzio, R.C. Piper, Mammalian late vacuole protein sorting orthologues participate in early endosomal fusion and interact with the cytoskeleton, Mol. Biol. Cell 15 (2004) 1197–1210.
[19] B.Y. Kim, Y. Sahara, A. Yamamoto, E. Kominami, S. Kohsaka, C. Akazawa, The interaction of mammalian Class C Vps with nSec-1/Munc18-a and syntaxin 1A, Biochem. Biophys. Res. Commun. 350 (2006) 691–697.
[20] R. Puertollano, Interaction of Tom1L1 with the multivesicular body sorting machinery, J. Biol. Chem. 280 (2005) 9258–9264.
[21] K.G. Bache, A. Brech, A. mehlum, H. Stenmark, Hrs regulates multivesicular body formation vis ESCRT recruitment to endosomes, J. Cell Biol. 162 (2003) 435–442.
[22] B.Y. Kim, J.A. Olzmann, G.S. Barsh, L.S. Chin, L. Li, Spongiform neurodegeneration associated E3 ligase Mahogunin ubiquitylates TSG101 and regulates endosomal trafficking, Mol. Biol. Cell 18 (2007) 1129–1142.
[23] A. Doyotte, R.G. Russell, C.R. Hopkins, P.G. Woodman, Depletion of TSG101 forms a mammalian Class E compartment: a multicisternal early endosome with multiple sorting defects, J. Cell Sci. 118 (2005) 3003–3017.
[24] K.G. Bache, T. Slagsvold, A. Cabezas, K.R. Rosendal, C. Raiborg, H. Stenmark, The growth-regulatory protein HCRP1/hVps37A is a subunit of mammalian ESCRT-1and mediates receptor down regulation, Mol. Biol. Cell 15 (2004) 4337–4346.
[25] S. Yogosawa, S. Hatakeyama, K.I. Nakayama, H. Miyoshi, S. Kohsaka, C. Akazawa, Ubiquitylation and degradation of serum-inducible kinase by hVps18, a RING-H2 type ubiquitin ligase, J. Biol. Chem. 280 (2005) 41619–41627.
[26] S. Yogosawa, M. Kawasaki, S. Wakatsuki, E. Kominami, Y. Shiba, K. Nakayama, S. Kohsaka, C. Akazawa, Biochem. Biophys. Res. Commun. 350 (2006) 82–90.

Please cite this article in press as: B.Y. Kim, C. Akazawa, Endosomal trafficking of EGFR regulated by hVps18 via ..., Biochem. Biophys. Res. Commun. (2007), doi:10.1016/j.bbrc.2007.08.046